Electronic Supplementary Material (ESI) for Journal of Materials Chemistry C.

Supporting information

High strength, stable and self-healing copolyimide for defects induced by mechanical and electrical damages

Baoquan Wan,[a] Xiaodi Dong,[a] Xing Yang,[a] Ming-Sheng Zheng,[*a] George Chen,[b] Jun-Wei Zha[*acd]

[a]School of Chemistry and Biological Engineering, University of Science and Technology Beijing, Beijing 100083, P. R. China
[b]Department of Electronics and Computer Science, University of Southampton, Southampton SO17 1BJ, UK
[c]Beijing Advanced Innovation Center for Materials Genome Engineering, University of Science and Technology Beijing, Beijing 100083, P. R. China
[d]Shunde Graduate School of University of Science and Technology Beijing, Foshan 528300, P.R. China

Corresponding authors
Prof. Jun-Wei Zha
E-mail: zhajw@ustb.edu.cn
Dr. Ming-Sheng Zheng
E-mail: zhengms@ustb.edu.cn

1. Polyimide (PI) and copolymerized polyimide (CPI) films

Firstly, the copolymerized polyimide (CPI) films with different large proportion of components were prepared to explore the self-healing effect of disulfide bond exchange in polyimide system. It is known that the CPI films with the copolymerization ratios of 4-Aminophenyl disulfide (APD) and 1,3-bis(4'-Aminophenoxyl) benzene (BAPB) of 10:0 and 7:3 has self-healing characteristics. Secondly, The CPI films with different small proportion components were synthesized again to study the mechanical and insulation properties before and after self-healing. The specific component changes are shown in **Table S1**.

Table S1. All proportional components of copolyimide.

Number of times	**CPI (APD: BAPB)**	**APD (mol)**	**BAPB (mol)**	**BPADA (mol)**
Group 1	10:0	3	0	3
	7:3	2.1	0.9	3
	5:5	1.5	1.5	3
	3:7	0.9	2.1	3
	0:10	0	3	3
Group 2	10:0	3	0	3
	9:1	2.7	0.3	3
	8:2	2.4	0.6	3
	7:3	2.1	0.9	3
	6:4	1.8	1.2	3

The molecular structures and synthesis conditions of polyimide (PI) are illustrated in **Fig. S1**. The purpose of thermal imidization of PI film precursors composed of disulfide bond monomers APD and 4,4'-(4,4'-isopropylidenediphenoxy) diphthalic anhydride (BPADA) under different temperature gradients is to synthesize PI with good film-forming effect.

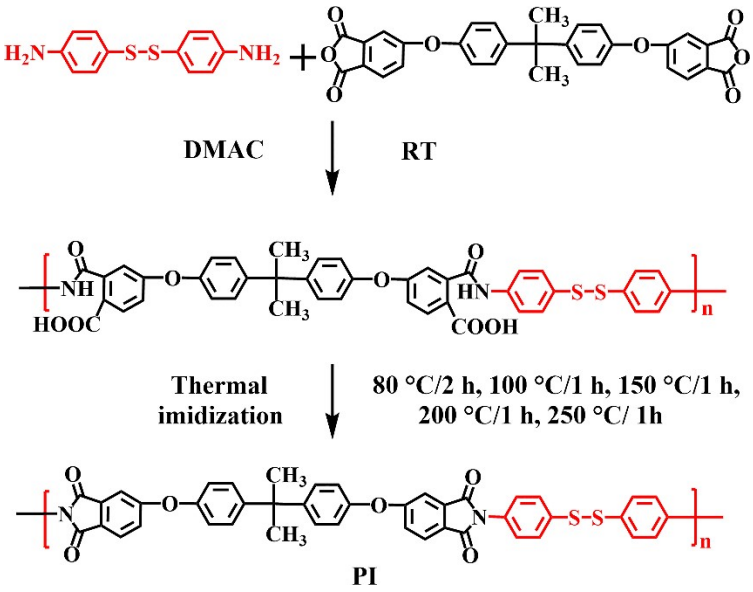

Fig. S1. Synthetic process and reaction conditions of PI precursor and PI.

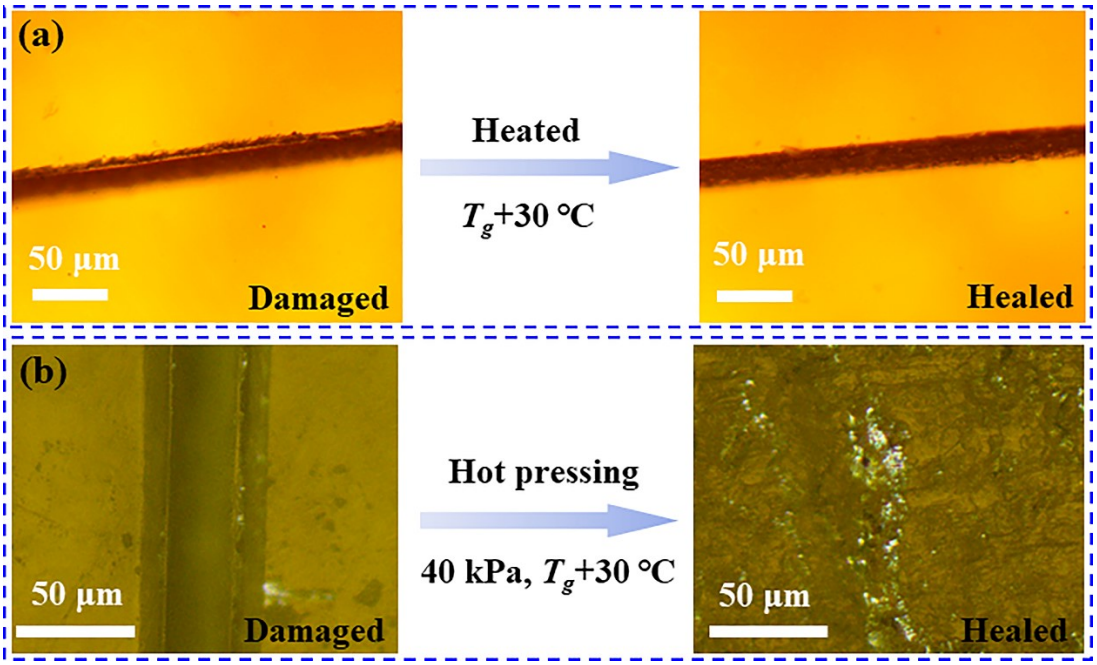

Fig. S2. Optical photos of damaged and healed PI (APD+BPADA) under different conditions.

Fig. S3 illustrates the molecular structures and synthesis conditions of CPI. In order to improve the mechanical and insulation properties of self-healing CPI, the copolymerization process is selected to prepare the CPI films with high temperature resistant and good insulation strength. Furthermore, the precursor of CPI film synthesized from disulfide bond, BAPB and BPADA monomers was thermally imidized as same as above.

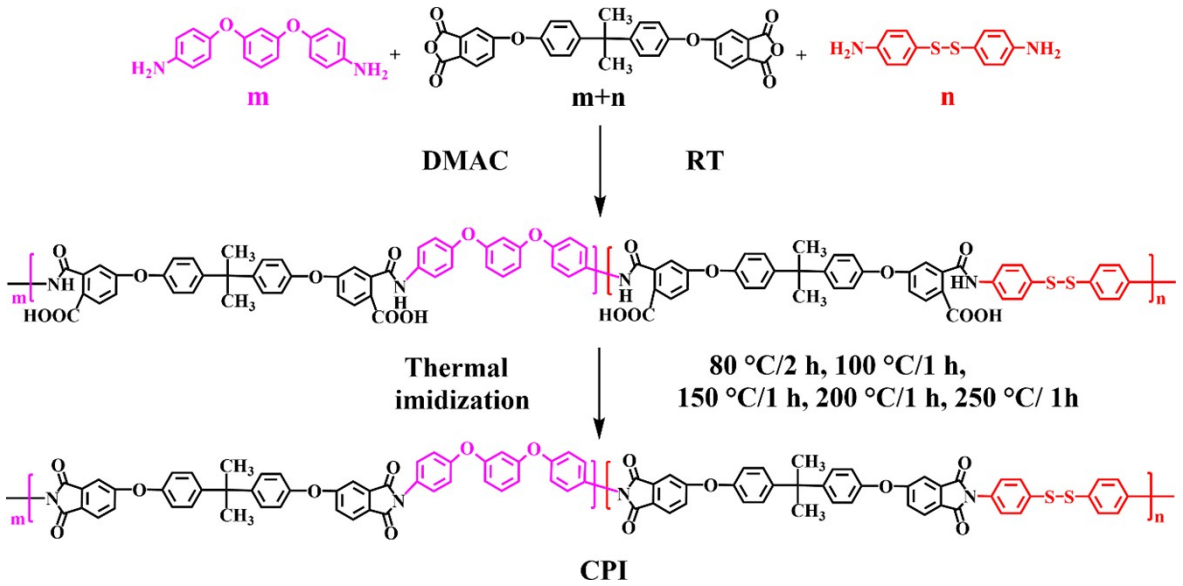

Fig. S3. Synthetic process and reaction conditions of CPI precursor and CPI.

The specific preparation process of PI or CPI films is shown in **Fig. S4**. The synthesized PI or CPI precursor solution was placed in a vacuum drying oven to eliminate bubbles. Moreover, the precursor solution is scraped on a clean glass plate with a manual film scraping machine. The glass plate with a layer of precursor solution is placed in a blast drying oven with temperature programmed function for thermal imidization reaction with different temperature gradients to synthesize PI or CPI with good film-forming effect.

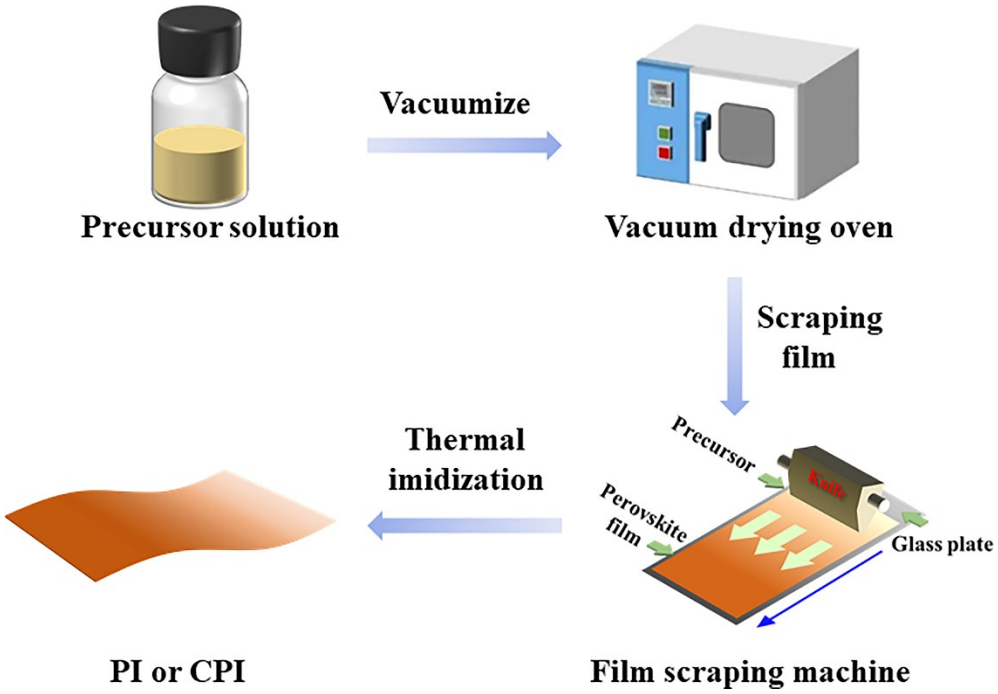

Fig. S4. The polymerization process of the PI and CPI.

2. Thermal, mechanical properties and breakdown strength of CPI films

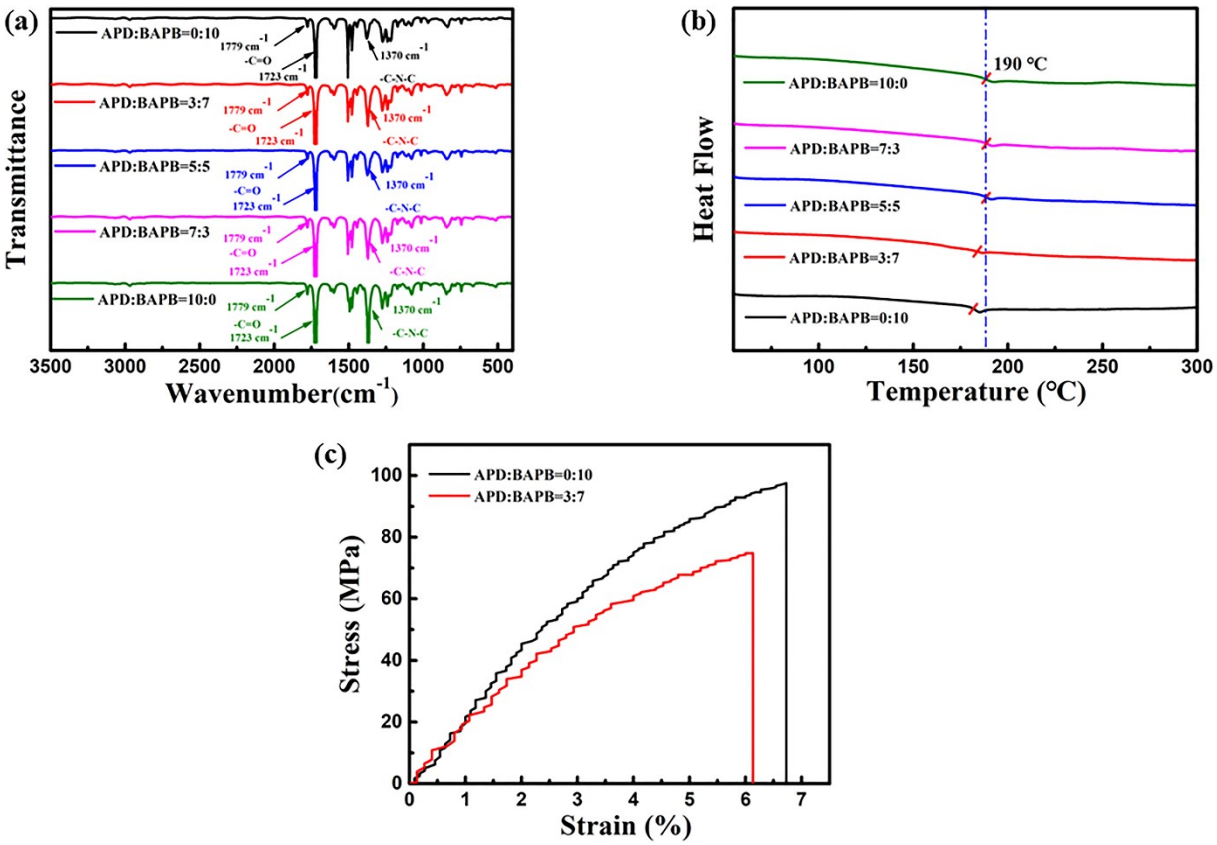

Fig. S5. (a) FT-IR patterns, (b) DSC curves, (c) stress-strain curves of the different proportion CPI films.

The Weibull distribution of breakdown strength of CPI films with large proportion of components is shown in **Fig. S6**. It can be found that with the increase of BAPB ratio, the breakdown strength of the CPI film increases continuously, up to 450 kV/mm. The reason may be that more benzene ring structures in BAPB are easy to form π-π conjugate structure in the process of molecular chain stacking. This structure helps to block the propagation path of electrical tree at the molecular level, so as to improve the breakdown.[1,2]

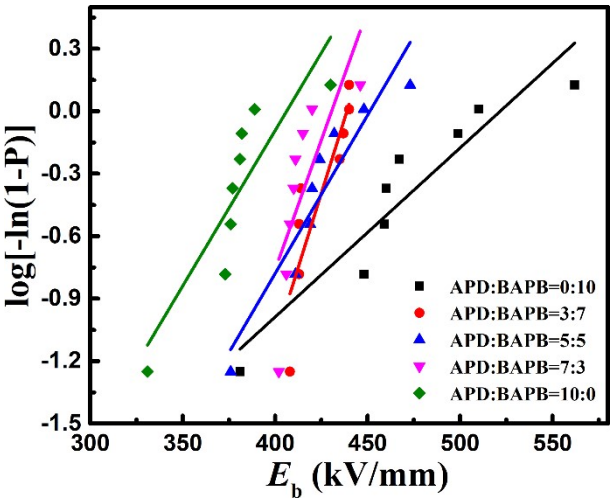

Fig. S6. Weibull distribution of breakdown strengths of CPI films.

3. Self-healing of CPI films

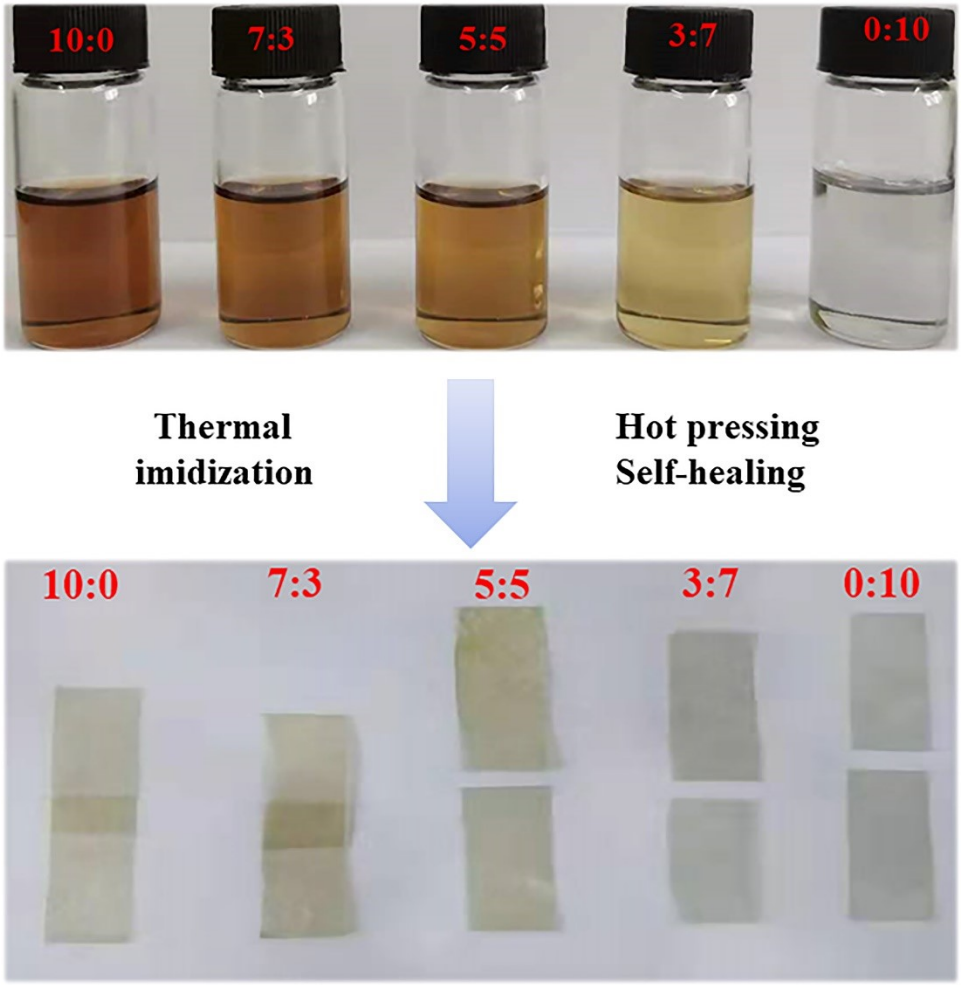

Fig. S7. Digital photos of CPI precursor solutions and repaired CPI films.

As shown in **Fig. S8**, the CPI films of different components are cut and then re bonded healed under the condition of hot pressing (20 kPa, 200 °C). Moreover, the healed films were tested for mechanical properties. However, the CPI films with the ratios of APD to BAPB of 8:2, 7:3 and 6:4 are analyzed not to have the repair efficiency to meet the needs. After the test of mechanical properties, the re failure point of the films with three different components is still the separation of the original failure position, rather than the new failure point different from the original failure point as the films with two components of 10:0 and 9:1. More BAPB doping will excessively reduce the content of disulfide bond per unit volume and increase the distance between disulfide bond and disulfide bond in the molecular chain. Moreover, more ethers will entangle during the movement of molecular chains. The above phenomena will hinder the exchange of disulfide bonds and reduce the self-healing efficiency.[3,4] Consequently, the films with the ratio of 10:0 and 9:1 are selected to study the self-healing ability after mechanical/electrical damage.

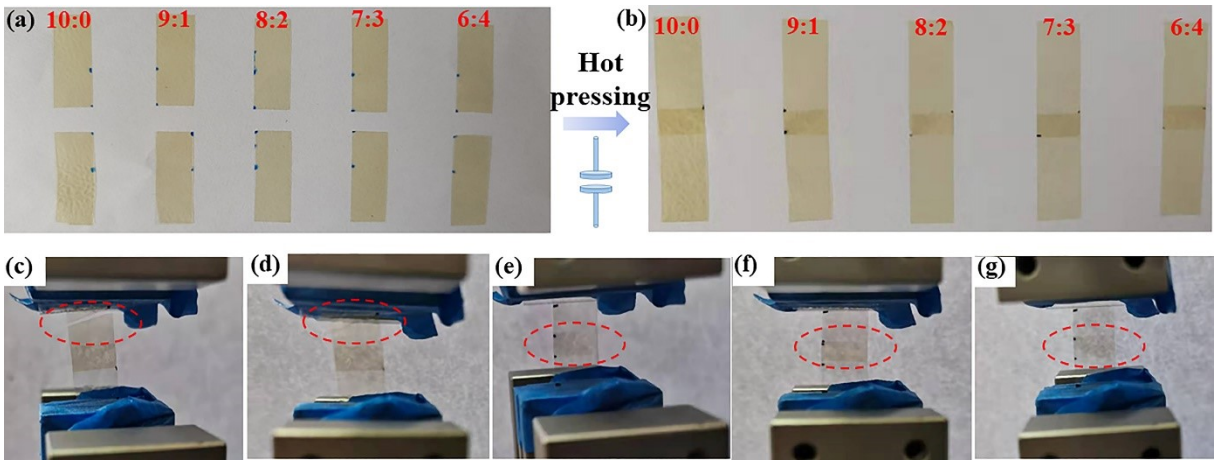

Fig. S8. Digital photos of (a) different proportions of films are cut, (b) different proportions of films are healed. Tensile test of CPI film with the ratio of APD to BAPB is (c) 10:0, (d) 9:1, (e) 8:2, (f) 7:3 and (g) 6:4.

Fig. S9 illustrates the optical microscope images of CPI films with three components of 8:2, 7:3 and 6:4 after being scratched and then self-healed. These CPI films cannot heal the cracks completely, which is different from the films with other two components. The reason may be that with the increase of BAPB ratio, the chain spacing between disulfide bonds increases, which hinders the mutual conversion between disulfide bonds to reduce the degree of self-healing.[5,6] Moreover, with the increase of BAPB ratio, the reduction of disulfide bond content is also a macro factor for the decrease of CPI self-healing efficiency.

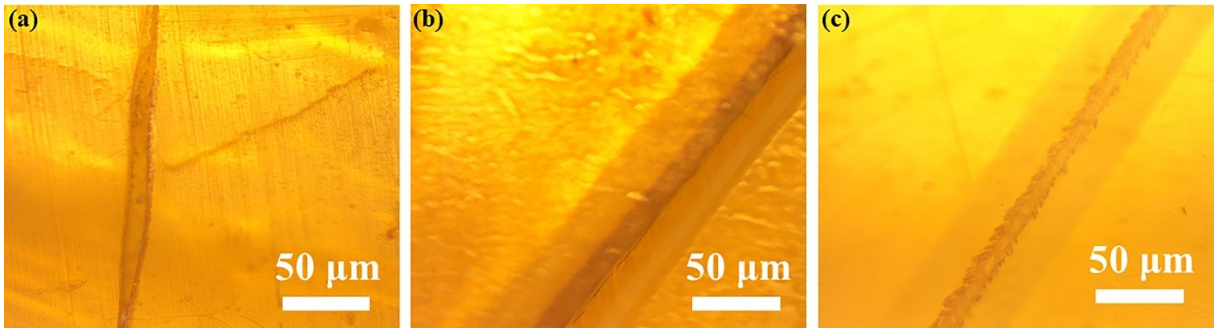

Fig. S9. Optical microscope image of the CPI films with the ratio of APD to BAPB is (a) 8:2, (b) 7:3 and (c) 6:4.

4. Self-healing efficiency of CPI films

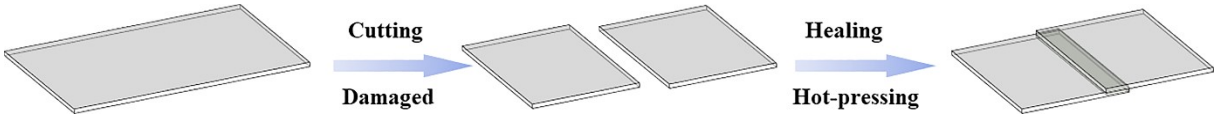

Fig. S10. Schematic diagram of CPI films dislocation self-healing process.

As shown in Fig. S10, the CPI films of different components are cut and then re bonded healed under the condition of hot press. Actually, the original CPI film is different from the self-healed film with mutual bonding (the thickness of the overlap of the film). Therefore, the self-healing efficiency of the film cannot be simply described by tensile strength or elongation at break. Comprehensively, physical quantities that can simultaneously describe the relationship between stress and strain are proposed to measure the self-healing efficiency of CPI.[7,8] Young's modulus (*E*) is defined as a physical quantity describing the relationship between stress and strain within the scope of Hooke's law, which can be used to measure the self-healing efficiency of CPI.[9] Within Hooke's law, the self-healing efficiency of CPI film is defined as: [10]

$$\eta = \frac{E_{healed}}{E_{original}} \times 100\%$$

Simultaneously, the self-healing efficiencies of CPI-100 and CPI-91 are as follows:

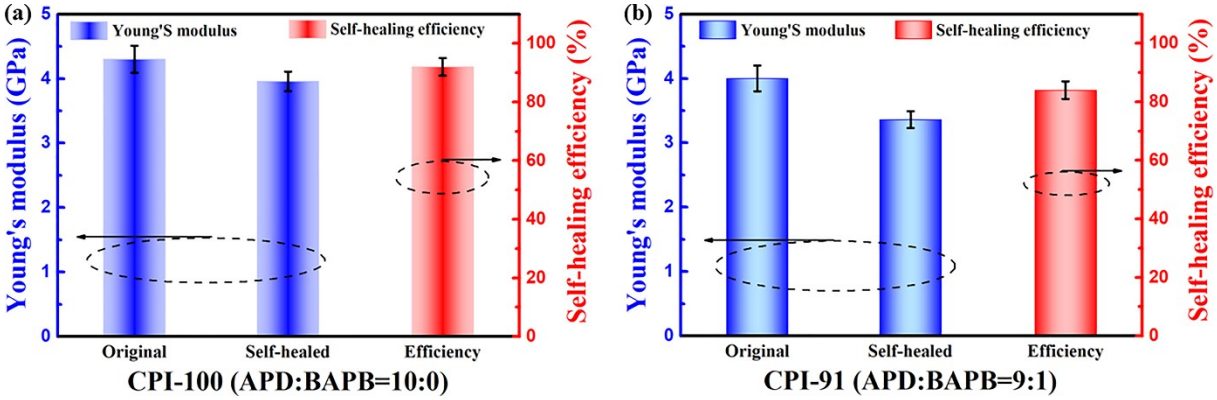

Fig. S11. (a) Histogram of Young's modulus before and after self-healing and self-healing efficiency of CPI-100 film. (b) Histogram of Young's modulus before and after self-healing and self-healing efficiency of CPI-91 film.

5. Self-healing influence mechanism

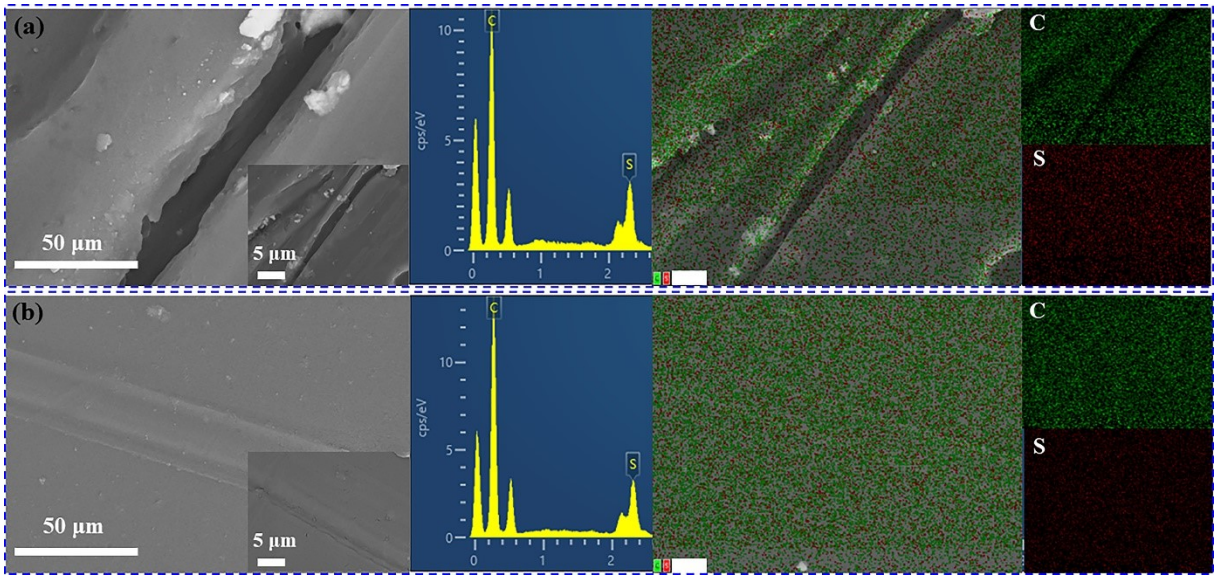

Fig. S12. Surface morphology and mapping (C, S elements) of (a) damaged and (b) self-healed CPI-100 film.

References

1 X. J. Liao, Y. C. Ding, L. L. Chen, W. Ye, J. Zhu, H. Fang, H. Q. Hou, Chem. Commun. 2015, 51, 10127–10130.

2 Y. L. Qiao, M. S. Islam, K. Han, E. Leonhardt, J. Y. Zhang, Q. Wang, H. J. Ploehn, C. B. Tang, Adv. Funct. Mater. 2013, 5, 5638–5646.

3 D. D. Li, C. Y. Wang, X. Y. Yan, S. Q. Ma, R. Lu, C. H. Chen, G. T. Qian, H. W. Zhou, RSC Adv. 2022, 12, 4234–4239.

4 D. Liu, J. W. Wang, W. H. Peng, X. Z. Wang, H. Ren, D. W. Kirk, React. Funct. Polym. 2022, 170, 105139.

5 Y. K. Saito, Y. Shichibu, K. Konishi, Nanoscale 2021, 13, 9971–9977.

6 J. C. Rong, J. Zhong, W. L. Yan, M. C. Liu, Y. L. Zhang, Y. L. Qiao, C. Q. Fu, F. Gao, L. Shen, H. F. He, Polymer 2021, 221, 123625.

7 A. Susa, A. Mordvinkin, K. Saalwächter, S. V. D. Zwaag, S. J. Garcia, Macromolecules 2018, 51, 8333–8345.

8 X. P. Li, R. Yu, Y. Y. He, Y. Zhang, X. Yang, X, J. Zhao, W. Huang, ACS Macro Lett. 2019, 8, 1511–1516.

9 L. X. Yang, L. B. Yang, R. L. Lowe, Mech. Mater. 2021, 157, 103839.

10 J. Z. Wang, M. Y. Li, Y. Q. Jiang, K. Yu, G. V. Hartland, G. P. Wang, J. Chem. Phys. 2021, 155, 144701.